

Establishment of an intragastric surgical model using C57BL/6 mice to study the vaccine efficacy of OMV-based immunogens against *Helicobacter pylori*

Sanjib Das, Prolay Halder, Soumalya Banerjee, Asish Kumar Mukhopadhyay, Shanta Dutta, Hemanta Koley*

Division of Bacteriology, ICMR-National Institute of Cholera and Enteric Diseases, P-33, CIT Road, Scheme-XM, Beliaghata, Kolkata-700010, India

*Corresponding author:

HemantaKoley, Scientist F, Division of Bacteriology, ICMR-National Institute of Cholera & Enteric Diseases, P-33, CIT Road, Scheme-XM, Beliaghata, Kolkata - 700010, India

E-mail: hemantakoley@hotmail.com/koleyh.niced@gov.in

Abstract

Chronic gastritis is one of the major symptoms of gastro-duodenal disorders typically induced by *Helicobacter pylori* (*H. pylori*). To date, no suitable model is available to study pathophysiology and therapeutic measures accurately. Here, we have presented a successful surgical infection model of *H. pylori*-induced gastritis in C57BL/6 mice that resembles features similar to human infection. The proposed model does not require any preparatory treatment other than surgical intervention. C57BL/6 mice were injected with wild-type SS1 (Sydney strain 1, reference strain) directly into the stomach. Seven days post infection, infected animals showed alterations in cytokine responses along with inflammatory cell infiltration in the lamina propria, depicting a prominent inflammatory response due to infection. To understand the immunogenicity and protective efficacy, the mice were immunized with outer membrane vesicles (OMVs) isolated from an indigenous strain with putative virulence factors of *H. pylori* [A61C (1), *cag+*/*vacA s1m1*]. In contrast to the non-immunized cohort, the OMV-immunized cohort showed a gradual increase in serum immunoglobulin(s) levels on the 35th day after the first immunization. This conferred protective immunity against subsequent challenge with the reference strain (SS1). Direct inoculation of *H. pylori* into the stomach influenced infection in a short time and, more

importantly, in a dose-dependent manner, indicating the usefulness of the developed model for pathophysiology, therapeutic and prophylactic studies.

Keywords: Animal model, Surgical intervention, Gastric illness, Outer membrane vesicles, Vaccine efficacy, *Helicobacter pylori*.

Background

Gastroduodenal disorders are the cumulative effect of carefully orchestrated molecular interactions between host and pathogen factors belonging to the genus *Helicobacter* [1]. With almost 50% of the population worldwide infected by the pathogen, it is one of the major health burdens in developing nations [2]. Although *H. pylori* has been recognized as a class I carcinogen by the WHO, very little has been explored thus far. This is primarily due to the asymptomatic nature of infected individuals, expensive clinical detection (e.g., endoscopy, urea breath test, etc.) and diagnosis with considerable information scarcity [3]. In addition to this, the global antimicrobial resistance (AMR) pattern of *H. pylori* is changing alarmingly, resulting in a paradigm shift in “treatment of choice” by clinical practitioner [4].

Research in *in vitro* and *in vivo* systems of *H. pylori* is continuously enriching our understanding of pathophysiology and genetic predisposition related to adaptation, survival and coevolution of the pathogen [5, 6]. For instance, *H. pylori* has the inherent ability to modulate the gastric microenvironment, such as increasing gastric pH by means of urease upregulation, employing different adhesion proteins or simply dislodging itself when the pH becomes overwhelmingly acidic [7,8]. Such responses, along with others, act as the precursor to a chronic infection that largely depends on the gastric acid neutralizing capacity unique to each strain. The pathogen is known to recruit different adhesins depending upon the stages of disease progression, such as BabA during early infection or SabA during ongoing inflammation [9]. In addition, host antigens present on the surface of host cells, mucins and other gastric cells, such as A/B-Le^b, MUC5AC, MUC1 and H type 1, play important roles in bacterial adhesion, further promoting the severity of different gastric maladies [10,11].

To date, a combination of antibiotics with a proton pump inhibitor (PPI) is the only mode of treatment available due to the lack of a potent vaccine [12]. Moreover, an efficient animal model is crucial to understanding the immunological attributes of different immunogen(s) for vaccine development, which existing models fail to satisfy. To date, considerable efforts have been made to establish a reliable murine (gerbil or mouse) model to serve this purpose, including extensive application of transgenic animals with single or double mutations, but unfortunately, no significant efforts have been made toward the route of administration to induce an infection [13]. The preexisting method relies on the oral administration of multiple doses of inoculums along with antibiotic pretreatment to induce an infection [14]. Moreover, it takes a minimum of two weeks to develop an infection using the traditional approach, which is significantly higher than any other enteric pathogens, such as *E. coli* or *Salmonella*, while using an animal model [15–17].

Therefore, in this study, we introduced an infection by surgically exposing the stomach of C57BL/6 mice and directly injecting *H. pylori* inoculums. We assessed different pathological and immunological markers for active infection and applied the same to study the vaccine efficacy of OMV-based immunogens isolated from a prevalent strain.

Methods

Bacterial strains and culture conditions

Bacterial strains were revived from glycerol stock using brain heart infusion agar (BD Difco, USA) supplemented with 7% horse blood, 0.4% IsoVitaleX with antibiotics such as amphotericin B, trimethoprim, and vancomycin (Sigma Aldrich, USA) at concentrations as described previously [18]. Inoculated plates were then kept under microaerophilic conditions (5% O₂, 10% CO₂, and 85% N₂ at 37°C) for 48 hrs and sub-cultured before conducting any experiment.

Broth culture was prepared using Brucella Broth (BD, Difco, USA) supplemented with 10% horse serum and vancomycin (Sigma, USA). The inoculated flask was then kept in shaking conditions (100 rpm) overnight while maintaining the microaerophilic environment [19].

Characterization and selection of strains

All strains were checked for oxidase, catalase and urease as mentioned elsewhere [20]. Next, an antibiogram was performed using the agar dilution method following CLSI guidelines (**Supplementary table:1**). PCR-based detection was applied for genotypic characterization. Some major virulence factors, such as *cagA*, *vacA*, *babA* and *dupA*, were checked using either simplex or multiplex PCR [21,22]. The primers used in the present study are listed in a table (**Supplementary table: 2**).

Animals

Six- to eight-week-old female C57BL/6 mice were received from the NICED-Animal house facility. The animals were kept in a condition maintained at $25\pm 2^{\circ}\text{C}$ with $65 \pm 2\%$ humidity and a 12/12-hour light/dark cycle. Animals weighing ~22 grams were selected for the study and provided with sterile food and water *ad libitum*. All experiments were performed following the standard operating procedure outlined by the Committee for the Purpose of Control and Supervision of Experiments on Animals (CPCSEA), Ministry of Environment and Forest, Government of India (CPCSEA Registration no. 68/GO/ReBi/S/1999/CPCSEA valid 17.07.2024) and Institutional Animal Ethics Committee (IAEC) of NICED was approved (Approval No. PRO/194/June 2022-25) and supervised experimental design and protocols from time to time.

Animal experimental design

Thirty-six C57BL/6 mice were randomly assigned into two major groups, each comprising 18 animals. To determine an infectious dose for the surgical model, the first set of mice was further divided into three subgroups and infected with a dose of either 1×10^8 (n=6) or 2×10^8 CFU/mL (n=6, each) along with PBS control (n=6). All groups were housed for one or two weeks under sterile conditions.

For immunological studies, the remaining 18 mice were separated into two groups as: non-immunized (NI) (n=6) and oral or i.p. immunized (IM) (n=6 in each group). An oral or

intraperitoneal immunization with 50 µg of OMVs dissolved in PBS was administered on days 0, 14, and 28. Blood was collected at different time points, and the serum was isolated and stored at -20°C for use in different immunological assays. For the protective efficacy study, both groups (IM and NI) were infected surgically on the 35th day post-first immunization and sacrificed 7 days post-infection (**Supplementary figure:1**).

Intragastric surgical model development

Experimental animals were kept in fasting conditions overnight with sterile water. Initially, animals were sedated by an intraperitoneal injection of a mixture of ketamine (87.5 mg/kg) and xylazine (12.5 mg/kg) [23]. The stomach was exposed through a 2-3 cm midline incision without compromising any major blood supply. A disposable syringe with a 26G needle containing 200 µl (~2x10⁸ CFU) of the inoculums in PBS was directly injected into the stomach. Hydration was maintained in the exposed stomach using sterile normal saline throughout the surgery. The stomach was placed back inside the abdominal cavity, and the incision was sutured back. The incision site was monitored for any infection and occasionally washed with 5% povidone-iodine (betadine) soaked in a sterile gauze for 72 hours [24]. Sterile food and water were provided to the animals once they regained consciousness (**Fig. 1**).

Post-Surgery observation

All infected mice were observed twice a day for 7 days. Physical parameters were checked along with stool consistency and the nature of mucus or blood (if any) present in the feces. Rectal swabs were taken daily and were subjected to RUT solution and spread-plate to observe the shedding of the organism. Isolated colonies (if any) were confirmed using a PCR-based technique. *H. pylori* infection augments the modulation of both pro- and anti-inflammatory cytokines in the host [25]. Therefore, IL-1β, TNFα, IFNγ, IL-6, IL-10 and IL-17 were tested using cytokine measuring kits (Invitrogen, USA) following the manufacturer's protocol. 50µl of serum samples from 0-day, 7-day- and 14-day-infected mice were used to quantify the inflammatory response after post-operational (OP) observation due to infection.

Immunogen preparation

Outer membrane vesicles (OMVs) were isolated from the *Helicobacter* strain [A61C (1), *cagA*+, *vacA s1m1*] following the methods described previously with slight modification [26]. In brief, BB broth (BD, Difco, USA) was inoculated with log phase ($OD_{600} \sim 0.6$) pre-culture of the respective strains and kept overnight in microaerophilic conditions under constant shaking (100 rpm) at 37°C. On the next day, centrifugation was performed consecutively first at 8000xg for 15 min at 4°C, followed by 30 min with same conditions. The supernatants were then filtered twice with 0.45 μm and 0.22 μm syringe filters (Millipore, USA). To prevent protein degradation, a protease inhibitor cocktail was incorporated into the filtrate and ultracentrifuged at 140,000 x g at 4°C for 4 hrs using a P27A-1004 rotor (Hitachi). A density gradient centrifugation allowed obtaining the purified OMVs. Protein content was measured using a Lowry protein estimation kit (Pierce, USA) and stored at -20°C until further use.

Characterization of the Outer Membrane Vesicles (OMVs)

Dynamic Light Scattering

Concentrated OMVs were diluted 10-fold to reach a concentration of 0.1 mg/mL. The hydrodynamic size of OMVs was measured using a Malvern Zetasizer ZS90 (Malvern Instruments, Germany) and analyzed using ZS Xplorer version 3.1.0.64 [27].

Transmission electron microscopy

Diluted OMVs were placed on a carbon-coated grid and left for 10-20 min for absorption. The samples were then washed twice with drops of Tris buffer solution. Excess fluid was soaked using blotting paper, followed by staining with 2% uranyl acetate and air drying. Finally, the OMV-coated grids were observed under a JEOL JEM 2100 HR (JEOL, Tokyo, Japan) [28].

LC/MS of OMVs and analyses

Proteins present in OMVs were used for digestion and reduced with 5 mM TCEP and further alkylated with 50 mM iodoacetamide and again digested with trypsin (1:50, trypsin/lysate ratio) for 16 h at 37°C. Digests were cleaned using a C18 silica cartridge to remove the salt and dried using a speed vac. The dried pellet was resuspended in buffer A (2% acetonitrile, 0.1% formic acid). Experiments were performed on an Easy-nlc-1000 system coupled with an Orbitrap

Exploris mass spectrometer. One microgram of peptide sample was loaded on a C18 column (15 cm, 3.0 μ m Acclaim PepMap, Thermo Fisher Scientific), separated with a 0–40% gradient of buffer B (80% acetonitrile, 0.1% formic acid at a flow rate of 500nl/min) and injected for MS analysis. LC gradients were run for 60 minutes. MS1 spectra were acquired in the Orbitrap (MaxIT = 25 ms, AGC target=300%; RF lens = 70%; R=60 K, mass range = 375–1500; profile data). Dynamic exclusion was employed for 30s, excluding all charge states for a given precursor. MS2 spectra were collected for the top 12 peptides. MS2 (Max IT= 22 ms, R= 15 K, AGC target 200%). All samples were processed, and the generated RAW files were analyzed with Proteome Discoverer (v2.5) against the UniProt organism database. For dual Sequest and Amanda searches, the precursor and fragment mass tolerances were set at 10 ppm and 0.02 Da, respectively. The protease used to generate peptides, i.e., Enzyme specificity was set for trypsin/P (cleavage at the C-terminus of “K/R: unless followed by “P”). Carbamidomethyl on cysteine as a fixed modification and oxidation of methionine and N-terminal acetylation were considered variable modifications for the database search.

Extraction of lipopolysaccharide (LPS) and outer membrane proteins (OMPs)

LPS and OMPs were extracted following the methods described earlier [29]. LPS was then treated with proteinase-K to ensure the absence of any protein residue. The carbohydrate content of LPS was then quantified using the phenol–sulfuric acid method and measured at a wavelength of 492 nm [30]. Isolated proteins were quantified for their concentration using a Modified Lowry’s Kit (Pierce, USA) and measured at 660 nm using a spectrophotometer.

ELISA

Serum immunoglobulin (IgG, IgM, IgA, IgG2c) levels were measured against OMPs or LPS following the method described previously [31]. Twofold serial dilutions were prepared from serum isolated from both immunized and non-immunized groups. HRP-conjugated secondary anti-mouse IgG, anti-IgA, anti-IgG2c and anti-IgM antibodies (Sigma Aldrich, USA) were used to detect the antibody titer. Each experiment was replicated thrice with pooled sera from different groups.

Serum Bactericidal Assay (SBA) and Scanning Electron Microscopy

The effect of immunized mouse sera on bacterial morphology was measured and visualized using scanning electron microscopy (SEM) following a previously described protocol [32]. Bacteria along with heat-inactivated mouse sera and 25% guinea pig complement (with/without) were incubated for 1 hr under microaerophilic conditions followed by plating for viable colonies or fixation with 3% glutaraldehyde overnight followed by a gradual dehydration step initially with alcohol and then substitution later with a mixture of alcohol and hexamethyldisilazane (HMDS) at ratios of 2:1, 1:1 and 1:2. Finally, the samples were mounted on specimen stubs, sputter-coated with gold and analyzed on a Quanta 200 SEM (FEI, Netherlands).

Cytokine assay

Both immunized and non-immunized mice were sacrificed, and the spleens were harvested. After isolating spleen cells; $\sim 10^5$ cells were cultured for two hours in RPMI1640 containing 10 % FBS incubated with 50 μg of OMVs and incubated overnight at 37°C (with 5 % CO₂) for 24 h. IL-10, IFN- γ , IL-1 β , IL-6, IL-4, TNF- α and IL-17 were measured in the culture supernatant using a cytokine measuring kit (Invitrogen, USA) [33].

Fluorescence-activated cell sorting (FACS) analysis

Spleen cells were harvested, cultured for two hours in RPMI1640 containing 10 % FBS and re-stimulated using isolated OMVs (50 μg) and incubated overnight at 37°C (with 5 % CO₂) for 24 h. The next day, the cells were scraped, washed thoroughly, blocked and then incubated with mouse anti-CD4⁺, CD8⁺ or CD19⁺ antibodies. Splenocytes were stained with anti-Mabs: CD4-phycoerythrin (PE), CD8 PE, CD19 PE or an isotype control PE (Miltenyi Biotec, USA). Unbound antibodies were washed, and a specific epitope of the immune cell population was observed using FACS Aria II [32].

Protective efficacy Study

Seven days after the last immunization, both the immunized and non-immunized groups were challenged with the wild-type SS1 strain using a newly developed surgical procedure and housed for 7 days before being sacrificed. The antrum of stomach of both immunized and non-immunized groups was isolated and separated into two parts. Half of each part was immediately

transferred to BHI kept on ice, and the other half was transferred to neutral buffered formalin (NBF, 10%) solution to fix the tissue and left at room temperature. Harvested tissue in BHI was weighed, homogenized and serially diluted using PBS. The diluted samples were then spread onto BHIA and kept under microaerophilic conditions for 3-5 days. Any visible colonies were then counted and confirmed using RUT and PCR. Histopathological assays were performed as described elsewhere [34,35]. Briefly, samples kept in 10% formalin were washed and gradually dehydrated using the alcohol gradation method followed by preparing a paraffin block. A thin section (approximately 5 μ m) was prepared using a microtome. The slides were then de-waxed, rehydrated, and stained. Hematoxylin-Eosin was used for the study because they enhance tissue or bacterial contrast. Finally, the slides were mounted and observed under a microscope. Histological scoring was assigned for each sample based on their morphological changes. The gastric tissue observed under a microscope revealed various degrees of gastritis, which was then categorized according to the Houston-updated Sydney System based on the infiltration of inflammatory cells within the lamina propria [36].

Statistical analysis

The presented data do not follow a normal distribution due to biological variations. Nonparametric tests were adopted for all data analyses. Triplicate data were expressed as the mean \pm SD (standard deviation) using GraphPad Prism version 5.02. Two-way analysis of variance (ANOVA) or the Mann–Whitney test (for animal data) was performed as per the requirements, and statistical significance was determined from the *P* values mentioned in the figure legends.

Results

Characterization and selection of *H. pylori* strains used in the study

A total of 12 strains including 3 reference strains and 9 clinical strains were checked for the presence or absence of major virulence genes i.e. cytotoxin-associated gene or *cagA* representing *cag* pathogenicity island (*cagPAI*), vacuolating toxin A or *vacA*, blood group antigen binding

adhesin 2 or *babA2* and duodenal ulcer promoting gene or *dupA*. A type I or type II strain is defined by the presence of *cag* and allelic variations of *vacA* with signal region (*s1* or *s2*) and middle region (*m1* or *m2*). A *cag+s1m1* is considered to be more virulent, thereby influencing diseases development than *cag+s2m2* or any combination of *s1*, *s2*, *m1* and *m2*. Additionally, allelic variations of *babA* i.e *babA2*, plays a key role in adhesion to the Lewis B (Le^b) antigen of blood as *babA1* is known to be non-functional [21]. *dupA* belongs to a plasticity region (*jhp0917-jhp0918*) and found to be responsible in developing ulcers in *H. pylori* infected individuals [66]. Therefore, any strain positive for all these genes can be considered to be more virulent than others. A61C (1) is positive for all these virulence genes and therefore is selected for immunogen preparation. However, for model establishment and challenge study purpose, SS1 is considered to be more suitable than others as it is a mouse adapted strain. The result of genetic characterizations of all strains is listed in a table (**Supplementary table: 3**).

Clinical response caused by surgical intervention

In the present study, 2×10^8 CFU of bacteria were used to induce an active infection. Oral inoculation with the aforementioned dose revealed inconsistent results. Moreover, in the majority of cases, very little or no recovery of the bacterial population was observed using available detection techniques. Mice receiving WTSS1 directly to their stomachs by surgical means developed various degrees of gastric changes. Recovery of bacterial colonies from stool was insignificant and erroneous compared to gastric tissues, which were considerably higher (~2-3 times) and were confirmed to be positive upon RUT, spread-plate and PCR. The recovery rate of *H. pylori* from the 7-day infected mice was comparatively higher than that at 14 days post infection (**Fig.2**).

Intragastric surgical evoked inflammatory response Cytokine analysis of intragastrically infected mice of different time points i.e. 0-day, 7 day, and 14 days, showed drastic differences in serum cytokine levels. IFN- γ , IL-1 β , TNF- α , IL-10, and IL-17 are increasing more on day 7 after infection and also reducing progressively on day 14. In case of IL-6, which is responsible

for sustaining inflammation is increasing on day 14. The majority of the pro-inflammatory cytokines were upregulated after 7 days post infection, except IL-6, which was found to be more pronounced at 14 days than at 7 days post infection (**Fig.3**) indicating active *H. pylori* infection.

Histopathological changes due to intragastric infection

Histopathological observation plays crucial role in *H. pylori* diagnosis. *H. pylori* infection causes local inflammation in gastric tissue marked by various degrees of inflammatory infiltration with substantial damage in gastric epithelium leading to the survival of the bacteria to the gastric microenvironment. Moreover, previous study has already showed a pronounced effect on gastric tissue of C57BL/6 mice upon *H. pylori* infection. Therefore, in order to establish a successful infection mediated by surgical intervention, stomach samples were taken at different time points and the topographical changes were compared. Negative control mice, receiving only PBS and Day0 had no inflammation (**Fig 4.i: a, b**) whereas inflammatory infiltration was significantly higher on day7 (**Fig 4.i:c**) compared to day 14(**Fig 4.i: d**). In addition to this, mucosal epithelium was severely damaged with exposed gastric pits in both cases. In contrast, metaplasia due to infection was more prominent on day 14 than day 7, indicating a successful infection. Histopathological scoring was assigned based on Sydney system (**Fig.4. ii**).

Isolation and characterization of OMVs from *H. pylori* strain A61C (1)

The OMVs isolated from the broth culture of A61C (1) were purified and assessed using dynamic light scattering (DLS), transmission electron microscopy (TEM) and proteomics analyses using LC/MS (**Fig. 5.A**). The data revealed uniformity in OMVs structure with a diameter of 50nm (**Fig. 5.B.i, ii**). TEM image showed the OMVs to be circular in shape with distinct bilayers. The protein components present in OMVs isolated from the immunogen strain [A61C (1)] revealed 18 major proteins including UreB, UreA, FtnA, GroEL, UbiX, Tuf, SecA, RplII, LpxK, RimO, AroB along with some other proteins with unknown localization (Fig. 5.C, **Supplementary table 4**). Presence of proteins like UreA, UreB and GroEL on OMVs indicate the potential to generate a strong immune response as these proteins are known for their

immunomodulatory activities. The sub-cellular localization of proteins indicated by the software includes cytoplasm, membrane, periplasmic space, plasma membrane of the bacteria. *H. pylori* LPS is known to have no cytotoxicity which is also evident from cytotoxicity assay (**Supplementary figure 2**).

***H. pylori* OMVs induce pro-inflammatory cytokine response**

35th day post immunization splenic cells were harvested from both immunized and non-immunized mice and re-stimulated with 50µg of OMVs. A significant induction in IFN-γ, TNF-α, IL-1β, IL-4, IL-10, IL-17, IL-6 and IL-12, IL-13 levels were observed (**Fig. 6.a-i**). Moreover, our data revealed oral immunization to be a better route for immunization as most of pro-inflammatory cytokines. Contrary to previous studies [63], our study did not find any Th1 or Th2 biased response indicating the immune response against OMVs is independent of routes of administration, compared to the control, both oral and i.p. immunized animals revealed elevation in cytokines. Altogether, immunization invoked an array of cytokines than non-immunized implying the potential of OMVs for a vaccine candidate.

Immunization of *H. pylori* OMVs elicited higher adaptive immune response

Previous studies on bacterial extracellular vesicles revealed OMVs to be an excellent vaccine candidate against bacterial pathogens [62]. OMVs are known to induce both humoral and cellular arms of immune responses usually mediated by outer membrane proteins (OMPs) and lipopolysaccharides (LPS). We investigated serum immunoglobulin levels (**Fig 7.A.i-iv**) of oral and intraperitoneally immunized mice and found significant difference compared to the control. However, we did not find significant differences between oral and intraperitoneal immunization.

Next, we evaluated the bactericidal activity of the immunized serum. The data showed significant reduction in bacterial number when immunized serum is incubated with 25% guinea pig serum as compared to non-immunized mice serum (**Supplementary figure 3**). This confers activation of complement mediated pathway, along with sufficient antibody titer in immunized

C57BL/6 mice that effectively kill the bacteria by damaging the bacterial surface as viewed under SEM (**Fig 7. C, D.i-ii**). Comparative analyses of the splenic cell population of immunized and non-immunized mice were done using a flow cytometer. Immunization with OMVs showed significantly higher population of CD4+, CD8a+ and CD19+ (**Fig 7. B**) cells indicating a strong immune response in immunized mice.

In all, immunization with *H. pylori* OMVs generated adaptive immune responses in C57BL/6 mice and significantly activated adaptive immune responses which could in turn help to provide long term protective immune response against infections caused by *H. pylori* (**Figure 7.A.iii-iv**).

Protective efficacy study post immunization

After immunization with OMVs, the immunized and non-immunized animals were challenged with wild type SS1 with a dose mentioned before (i.e. 2×10^8 CFU) and the colonization were analyzed 7 days post infection. A significant decrease in colonization was observed in the stomach tissue of immunized than non-immunized animals indicating a substantial reduction in bacterial load (**Fig. 8.D**). To confirm further, DNA was extracted from the gastric tissue and subjected to *ureB* PCR for the presence of *H. pylori*. All non-immunized mice were found to be positive whereas immunized animals were found insignificant presence - of *H. pylori* DNA among OMVs immunized animals (**Fig. 8.C**). Histopathological changes of both immunized and non-immunized mice stomachs were analyzed 7 days post infection using surgical intervention (**Fig. 8.A.i-ii**). OMVs immunized mice showed a significant reduction in gastric epithelial damage, altered gastric mucosa, inflammatory infiltration, exposed gastric pit, and metaplasia. Pathological scores were also less in immunized mice than non-immunized mice (**Fig. 8.B**). Overall, reductions in bacterial numbers were observed upon immunization.

Discussion:

Over the years, a number of animal models have been evaluated for pathophysiology or treatment against *H. pylori*, including gnotobiotic pigs, dogs, cats, Mongolian gerbils, guinea

pigs, rhesus monkeys, and mice [37–48]. In most cases, C57BL/6 or black mice were explored extensively because of their substantial contribution in *H. pylori*-related studies. The proper route for administering the pathogen and/or immunization also has a key impact on the development of an infection and assessment of immune response, which is another important consideration when selecting an animal model for *in vivo* studies. Therefore, cytokine alterations along with histological changes described in the present study represent a successful infection achieved through our newly developed surgical model. Conventional approaches for studying *H. pylori* infection in animals usually involve multiple oral inoculations using an oral gavage [49–51]. However, relying solely on the oral route to induce an infection and expecting the bacterium to outcompete the existing microflora and successfully colonize the stomach may not always yield a consistent result in any given experimental setting. This can cost significant time and resources being invested while still fostering uncertainty about an actual infective status in experimental animals. Therefore, it is important to consider the limitations and variability of the *in vivo* systems and look for alternative approaches that could provide a more reliable method of *H. pylori*-mediated pathogenesis in animal models. Clinical detection of *H. pylori* infection generally involves histology and PCR apart from the Rapid Urease Test (RUT) [52–54]. Serological tests are often avoided, as previously invoked antibodies fail to recognize the actual infective status of recent manifestations [55, 56]. As a consequence, this increases the chances of false positive results. In addition, histology allows visualization of pathogen-induced changes in gastric tissues, such as the intensity of inflammatory cell infiltration or aberrations in gastric topology, while PCR detects the presence of genomic DNA of *H. pylori* in gastric tissue samples [57]. However, it should be noted that neither histological observations nor negative PCR results rule out the presence of an infection [58]. Thus, a number of different techniques must be employed simultaneously to achieve a more accurate diagnosis of *H. pylori* infection [59]. Our study comprised a combination of histological observation, PCR detection and quantification of serum cytokine levels to confirm active *H. pylori* infection.

Surgical intervention initially spiked pro-inflammatory cytokines such as IFN- γ and IL-1 β along with IL-17 significantly more on day7 than on day14. However, as the infection progressed, these cytokines were lowered and finally balanced, except for IL-6, which was found to be elevated more on day 14 than on day 7. A pronounced IL-6 level at later stages might indicate ongoing inflammation in the gastric lining with potentially developing chronic gastritis. Such

responses were further supported by the induction of other cytokines. IFN- γ is an early effector molecule responsible for generating a Th1-mediated response by initiating different signaling cascades. However, up-regulation of IFN- γ transiently down-regulates IL-1 β production. In addition, IL-17, a cytokine regulating the Th-17-based response, plays important roles in both pathogenesis and host immunity. Studies with chronic diseases have revealed that well-balanced IL-1 β and IL-17 levels are constitutively produced to sustain inflammation due to infection in the long term [67]. In the case of *H. pylori* infection, both IL-1 β and IL-17 play crucial roles in pathogenesis; in particular, IL-17 influences the disease outcome upon infection. Our model showed an initial elevation in these cytokines, which decreased over time, indicating progression toward a chronic infection. However, as 7 days were not sufficient to develop a chronic infection, our model showed promising results in a time-dependent manner. Consistent with the cytokine analysis, histopathological observations also validate such changes to some extent. Intense inflammatory cell infiltration was observed on day 7 than on day 14, and the gastric lining was found to be more damaged with exposed gastric pits, indicating destruction caused by bacteria. Nevertheless, we did not find any striking structural abnormalities in gastric tissue 7 days post infection. PCR results from the same samples confirmed the presence of bacterial genomic DNA in experimental animals.

Next, we evaluated the surgical model for vaccine efficacy studies. Two different immunization routes were assessed to observe any alterations in the immune response due to changes in the route of administration. Immunization was performed both orally and intraperitoneally (i.p.) on days 0, 14 and 28. Initially, an elevation of serum IgG, IgM and IgA levels was observed against OMPs but not LPS of *H. pylori*. This can be due to the structural similarity between *H. pylori* LPS and blood antigens of the host [60-61]. Furthermore, we evaluated IgG2c (IgG subtype) and found it to be increased in immunized rather than non-immunized groups [62]. Our study found oral immunization to be better responsive than i.p. route, which can be due to the presence of different surface proteins on OMVs that are more readily absorbed and reactive to gastric epithelial cells than peritoneal immune cells. A splenic cell re-stimulation (ex vivo) assay revealed enhanced Th2-based cytokine responses, such as IL-4, IL-13, IL-10 and IL-12, coinciding with previous studies with *H. pylori*-derived OMVs used as immunogens [63]. Interestingly, our study did not find any biased immune response against OMVs, indicating that the immune response to OMVs is not general but rather unique to each strain. CD4+, CD8a+ and

CD19+ cell populations were increased due to OMV immunization independent of the route of administration. OMV immunization ultimately leads to a reduction in bacterial colonization in immunized animals but not in non-immunized animals. Serum bactericidal assay (SBA) typically denotes the functional aspect of immunogen-invoked antibody response in killing the bacterial population via complement mediated pathway. This in-vitro method involves incubation of bacteria in presence of heat-inactivated serum isolated from both OMVs immunized and PBS immunized mice. Antibodies generated in host due to immunization are sufficient enough to reduce the bacterial CFU by means of agglutination as demonstrated in OMVs induced immune response against *S. Typhi* and *Paratyphi A* [31]. However, agglutination doesn't directly imply a bacteriostatic or bactericidal activity of the antibodies. Therefore, addition of purified baby rabbit [64] or guinea-pig [65] complement externally to these antibodies ensured the lysis of the bacteria via complement-mediated pathway. In the present study, incubation of bacteria treated with OMVs immunized or PBS immunized sera in presence of guinea-pig complement lead to significant reduction in viable colony numbers in immunized compared to the PBS immunized mice groups.

Conclusion

In conclusion, the intragastric surgical model of *H. pylori* infection can be used to study the pathophysiology, immune response, and potential therapies for *H. pylori* infection. Our study indicates that a minimum of 7 days is enough to develop an infection in this model. All experimental results showed that tissue samples collected at 7days post infection can provide better results for diagnosing *H. pylori* infection than samples obtained at 14 days post infection, as histological changes and inflammatory cell infiltration are typically more pronounced at earlier time points post infection. Moreover, the cytokine response and antibody generation further support this model for vaccine efficacy studies. The immunization of mice with *H. pylori* OMVs has been shown to reduce the bacterial load with elevated antibody titers and protect gastric tissue from destruction. Therefore, the intragastric surgical model can become a valuable tool for understanding the pathophysiology of *H. pylori* infection, formulation and evaluation of potent vaccine candidates and development of potential therapeutics.

Author contributions

Sanjib Das: Conceptualization, experimental design and performance, data analysis and interpretation, manuscript preparation, **Prolay Halder:** Experiment performed, data analysis and interpretation, review and edit manuscript, **Soumalya Banerjee:** Experiment performed, data analysis and interpretation, review and edit manuscript, **Asish Kumar Mukhopadhyay:** Review and edit manuscript, **Shanta Dutta:** Review and edit manuscript, **Hemanta Koley:** Conceptualization, experimental design and supervision, data analysis and interpretation, manuscript preparation, funding acquisition.

Acknowledgments

Our heartfelt thanks go to Mr. Suhashit Ranjan Ghosh, Mr. Subrata Singha, Mr. Pritam Nandy, and Mrs. Arpita Sarbajana for their technical assistance from time to time. We extend our gratitude to the University Grants Commission (UGC), New Delhi, India, for providing the fellowships to Sanjib Das under the CSIR-UGC-NFSC scheme (Student ID: SANJIB DAS under UGC-NFSC scheme 3363/(CSIR-UGCNETJUNE2018)), the Indian Council of Medical Research for providing the fellowship to Prolay Halder [Fellowship ID: ICMR-3/1/3/JRF-2018/HRD-066(66125)] and Soumalya Banerjee under the CSIR-UGC-NET scheme [StudentID:191620007740].

Conflict of interest

The authors declare no conflicts of interest.

Funding

This work was supported by the Indian Council of Medical Research as an ICMR-extramural project (Project Index No. VIR/20/2020/ECD-I).

References

1. Beswick EJ, Suarez G, Reyes VE. H pylori and host interactions that influence pathogenesis. *World JGastroenterol WJG*. 2006;12(35):5599-5605. doi:10.3748/wjg.v12.i35.5599
2. Salih BA. Helicobacter pylori Infection in Developing Countries: The Burden for How Long? *Saudi JGastroenterol Off J Saudi Gastroenterol Assoc*. 2009;15(3):201-207. doi:10.4103/1319-3767.54743
3. Graham DY, Malaty HM, Evans DG, Evans DJ, Klein PD, Adam E. Epidemiology of Helicobacter pylori in an asymptomatic population in the United States: Effect of age, race, and socioeconomic status. *Gastroenterology*. 1991;100(6):1495-1501. doi:10.1016/0016-5085(91)90644-Z
4. Sukri A, Lopes BS, Hanafiah A. The Emergence of Multidrug-Resistant Helicobacter pylori in Southeast Asia: A Systematic Review on the Trends and Intervention Strategies Using Antimicrobial Peptides. *Antibiotics*. 2021;10(9):1061. doi:10.3390/antibiotics10091061
5. Abadi ATB. Strategies used by helicobacter pylori to establish persistent infection. *World JGastroenterol*. 2017;23(16):2870-2882. doi:10.3748/wjg.v23.i16.2870
6. Kusters JG, van Vliet AHM, Kuipers EJ. Pathogenesis of Helicobacter pylori Infection. *ClinMicrobiol Rev*. 2006;19(3):449-490. doi:10.1128/CMR.00054-05
7. Mobley HLT. Urease. In: Mobley HL, Mendz GL, Hazell SL, eds. *Helicobacter Pylori: Physiology and Genetics*. ASM Press; 2001. Accessed April 24, 2023. <http://www.ncbi.nlm.nih.gov/books/NBK2417/>
8. Bugaytsova JA, Björnham O, Chernov YA, et al. Helicobacter pylori Adapts to Chronic Infection and Gastric Disease via pH-Responsive BabA-Mediated Adherence. *Cell Host Microbe*. 2017;21(3):376-389. doi:10.1016/j.chom.2017.02.013
9. Doohan D, Rezkitha YAA, Waskito LA, Yamaoka Y, Miftahussurur M. Helicobacter pylori BabA–SabA Key Roles in the Adherence Phase: The Synergic Mechanism for Successful Colonization and Disease Development. *Toxins*. 2021;13(7):485. doi:10.3390/toxins13070485
10. Niv Y. Helicobacter pylori and gastric mucin expression: A systematic review and meta-analysis. *World JGastroenterol WJG*. 2015;21(31):9430-9436. doi:10.3748/wjg.v21.i31.9430
11. Celli JP, Turner BS, Afdhal NH, et al. Helicobacter pylori moves through mucus by reducing mucin viscoelasticity. *Proc Natl Acad Sci*. 2009;106(34):14321-14326. doi:10.1073/pnas.0903438106
12. Status of vaccine research and development for Helicobacter pylori - PubMed. Accessed April 6, 2023. <https://pubmed.ncbi.nlm.nih.gov/29627231/>

13. Toyoda T, Yamamoto M, Takasu S, Ogawa K, Tatematsu M, Tsukamoto T. Molecular Mechanism of Gastric Carcinogenesis in *Helicobacter pylori*-Infected Rodent Models. *Diseases*. 2014;2(2):168-186. doi:10.3390/diseases2020168
14. A Mouse Model of *Helicobacter pylori* Infection | SpringerLink. Accessed April 24, 2023. https://link.springer.com/protocol/10.1007/978-1-0716-1302-3_14
15. He XH, Ouyang DY, Xu LH. Injection of *Escherichia coli* to Induce Sepsis. *Methods Mol Biol Clifton NJ*. 2021;2321:43-51. doi:10.1007/978-1-0716-1488-4_5
16. A Mouse Infection Model with a Wildtype *Salmonella enterica* Serovar Typhimurium Strain for the Analysis of Inflammatory Innate Immune Cells. Accessed April 24, 2023. <https://en.bioprotocol.org/en/bpdetail?id=4378&type=0>
17. Werawatganon D. Simple animal model of *Helicobacter pylori* infection. *World J Gastroenterol WJG*. 2014;20(21):6420-6424. doi:10.3748/wjg.v20.i21.6420
18. Patra R, Chattopadhyay S, De R, et al. Multiple Infection and Microdiversity among *Helicobacter pylori* Isolates in a Single Host in India. *PLoS ONE*. 2012;7(8):e43370. doi:10.1371/journal.pone.0043370
19. (PDF) Successful Culture Techniques for *Helicobacter* Species: General Culture Techniques for *Helicobacter pylori*. Accessed April 27, 2023. https://www.researchgate.net/publication/231214985_Successful_Culture_Techniques_for_Helicobacter_Species_General_Culture_Techniques_for_Helicobacter_pylori
20. Chattopadhyay S, Patra R, Ramamurthy T, et al. Multiplex PCR Assay for Rapid Detection and Genotyping of *Helicobacter pylori* Directly from Biopsy Specimens. *J Clin Microbiol*. 2004;42(6):2821-2824. doi:10.1128/JCM.42.6.2821-2824.2004
21. Ghosh P, Sarkar A, Ganguly M, et al. *Helicobacter pylori* strains harboring babA2 from Indian sub population are associated with increased virulence in ex vivo study. *Gut Pathog*. 2016;8:1. doi:10.1186/s13099-015-0083-z
22. El-Sayed MS, Musa N, Eltabbakh M, et al. Detection of *Helicobacter pylori* oipA and dupA genes among dyspeptic patients with chronic gastritis. *Alex J Med*. 2020;56(1):105-110. doi:10.1080/20905068.2020.1780675
23. Anesthesia (Guideline) | Vertebrate Animal Research. Accessed September 23, 2023. <https://animal.research.uiowa.edu/iacuc-guidelines-anesthesia>
24. Soumik Barman, Dhira Rani Saha, Thandavarayan Ramamurthy, Hemanta Koley, Development of a new guinea-pig model of shigellosis, *FEMS Immunology & Medical Microbiology*, Volume 62, Issue 3, August 2011, Pages 304–314, <https://doi.org/10.1111/j.1574-695X.2011.00810.x>

25. Jan I, Rather RA, Mushtaq I, et al. Helicobacter pylori Subdues Cytokine Signaling to Alter Mucosal Inflammation via Hypermethylation of Suppressor of Cytokine Signaling 1 Gene During Gastric Carcinogenesis. *Front Oncol.* 2021;10. Accessed May 1, 2023. <https://www.frontiersin.org/articles/10.3389/fonc.2020.604747>
26. Bhaumik U, Halder P, Howlader DR, et al. A tetravalent Shigella Outer Membrane Vesicles based candidate vaccine offered cross-protection against all the serogroups of Shigella in adult mice. *Microbes Infect.* Published online January 22, 2023:105100. doi:10.1016/j.micinf.2023.105100
27. Choi HI, Choi JP, Seo J, et al. Helicobacter pylori-derived extracellular vesicles increased in the gastric juices of gastric adenocarcinoma patients and induced inflammation mainly via specific targeting of gastric epithelial cells. *ExpMol Med.* 2017;49(5):e330. doi:10.1038/emm.2017.47
28. Melo J, Pinto V, Fernandes T, et al. Isolation Method and Characterization of Outer Membranes Vesicles of Helicobacter pylori Grown in a Chemically Defined Medium. *Front Microbiol.* 2021;12. Accessed April 27, 2023. <https://www.frontiersin.org/articles/10.3389/fmicb.2021.654193>
29. Mukherjee P, Raychaudhuri S, Nag D, et al. Evaluation of immunogenicity and protective efficacy of combination heat-killed immunogens from three entero-invasive bacteria in rabbit model. *Immunobiology.* 2016;221(8):918-926. doi:10.1016/j.imbio.2016.03.002
30. DuBois Michel, Gilles KA, Hamilton JK, Rebers PA, Smith Fred. Colorimetric Method for Determination of Sugars and Related Substances. *Anal Chem.* 1956;28(3):350-356. doi:10.1021/ac60111a017
31. Howlader DR, Koley H, Sinha R, et al. Development of a novel S. Typhi and Paratyphi A outer membrane vesicles based bivalent vaccine against enteric fever. *PLoS ONE.* 2018;13(9):e0203631. doi:10.1371/journal.pone.0203631
32. Maiti S, Howlader DR, Halder P, et al. Bivalent nontyphoidal Salmonella outer membrane vesicles immunized mice sera confer passive protection against gastroenteritis in a suckling mice model. *Vaccine.* 2021;39(2):380-393. doi:10.1016/j.vaccine.2020.11.040
33. Helicobacter pylori Outer Membrane Vesicles Modulate Proliferation and Interleukin-8 Production by Gastric Epithelial Cells - PMC. Accessed April 6, 2023. <https://www.ncbi.nlm.nih.gov/pmc/articles/PMC201067/>
34. Kim N, Park YH. Atrophic Gastritis and Intestinal Metaplasia. In: Kim N, ed. *Helicobacter Pylori.* Springer; 2016:187-206. doi:10.1007/978-981-287-706-2_17
35. Hassan TMM, Al-Najjar SI, Al-Zahrani IH, Alanazi FIB, Alotibi MG. Helicobacter pylori chronic gastritis updated Sydney grading in relation to endoscopic findings and H. pylori IgG antibody: diagnostic methods. *J Microsc Ultrastruct.* 2016;4(4):167-174. doi:10.1016/j.jmau.2016.03.004

36. Björkholm BM, Guruge JL, Oh JD, et al. Colonization of Germ-free Transgenic Mice with Genotyped *Helicobacter pylori* Strains from a Case–Control Study of Gastric Cancer Reveals a Correlation between Host Responses and HsdS Components of Type I Restriction-Modification Systems*210. *J Biol Chem*. 2002;277(37):34191-34197. doi:10.1074/jbc.M203613200
37. Eaton KA, Ringler SS, Krakowka S. Vaccination of gnotobiotic piglets against *Helicobacter pylori*. *J Infect Dis*. 1998;178(5):1399-1405. doi:10.1086/314463
38. Krakowka S, Eaton KA, Leunk RD. Antimicrobial Therapies for *Helicobacter pylori* Infection in Gnotobiotic Piglets. *Antimicrob Agents Chemother*. 1998;42(7):1549-1554.
39. Neiger R, Simpson KW. *Helicobacter* Infection in Dogs and Cats: Facts and Fiction. *J Vet Intern Med*. 2000;14(2):125-133. doi:10.1111/j.1939-1676.2000.tb02225.x
40. Watanabe T, Tada M, Nagai H, Sasaki S, Nakao M. *Helicobacter pylori* infection induces gastric cancer in mongolian gerbils. *Gastroenterology*. 1998;115(3):642-648. doi:10.1016/s0016-5085(98)70143-x
41. Wu C, Shi Y, Guo H, et al. Protection against *Helicobacter pylori* infection in mongolian gerbil by intragastric or intramuscular administration of *H. pylori* multicomponent vaccine. *Helicobacter*. 2008;13(3):191-199. doi:10.1111/j.1523-5378.2008.00609.x
42. Sturegård E, Sjunnesson H, Ho B, et al. Severe gastritis in guinea-pigs infected with *Helicobacter pylori*. *J Med Microbiol*. 1998;47(12):1123-1129. doi:10.1099/00222615-47-12-1123
43. Shomer NH, Dangler CA, Whary MT, Fox JG. Experimental *Helicobacter pylori* Infection Induces Antral Gastritis and Gastric Mucosa-Associated Lymphoid Tissue in Guinea Pigs. *Infect Immun*. 1998;66(6):2614-2618.
44. Solnick JV, Chang K, Canfield DR, Parsonnet J. Natural Acquisition of *Helicobacter pylori* Infection in Newborn Rhesus Macaques. *J Clin Microbiol*. 2003;41(12):5511-5516. doi:10.1128/JCM.41.12.5511-5516.2003
45. Solnick JV, Fong J, Hansen LM, Chang K, Canfield DR, Parsonnet J. Acquisition of *Helicobacter pylori* Infection in Rhesus Macaques Is Most Consistent with Oral-Oral Transmission. *J Clin Microbiol*. 2006;44(10):3799-3803. doi:10.1128/JCM.01482-06
46. Metallic Nanoparticles as promising tools to eradicate *H. pylori*: A comprehensive review on recent advancements - ScienceDirect. Accessed August 22, 2023. <https://www.sciencedirect.com/science/article/pii/S2666831922000467>
47. Panthel K, Faller G, Haas R. Colonization of C57BL/6J and BALB/c Wild-Type and Knockout Mice with *Helicobacter pylori*: Effect of Vaccination and Implications for Innate and Acquired Immunity. *Infect Immun*. 2003;71(2):794-800. doi:10.1128/IAI.71.2.794-800.2003

48. Pan X, Ke H, Niu X, Li S, Lv J, Pan L. Protection Against *Helicobacter pylori* Infection in BALB/c Mouse Model by Oral Administration of Multivalent Epitope-Based Vaccine of Cholera Toxin B Subunit-HUUC. *Front Immunol*. 2018;9. Accessed August 22, 2023. <https://www.frontiersin.org/articles/10.3389/fimmu.2018.01003>
49. Nedrud JG. Animal models for gastric *Helicobacter* immunology and vaccine studies. *FEMS Immunol Med Microbiol*. 1999;24(2):243-250. doi:10.1111/j.1574-695X.1999.tb01290.x
50. Werawatganon D. Simple animal model of *Helicobacter pylori* infection. *World J Gastroenterol WJG*. 2014;20(21):6420-6424. doi:10.3748/wjg.v20.i21.6420
51. Taylor NS, Fox JG. Animal Models of *Helicobacter*-Induced Disease: Methods to Successfully Infect the Mouse. *Methods Mol Biol Clifton NJ*. 2012;921:131-142. doi:10.1007/978-1-62703-005-2_18
52. Guo BP, Mekalanos JJ. Rapid genetic analysis of *Helicobacter pylori* gastric mucosal colonization in suckling mice. *Proc Natl Acad Sci*. 2002;99(12):8354-8359. doi:10.1073/pnas.122244899
53. Mobley HLT. Urease. In: Mobley HL, Mendz GL, Hazell SL, eds. *Helicobacter Pylori: Physiology and Genetics*. ASM Press; 2001. Accessed April 24, 2023. <http://www.ncbi.nlm.nih.gov/books/NBK2417/>
54. Lee JY, Kim N. Diagnosis of *Helicobacter pylori* by invasive test: histology. *Ann Transl Med*. 2015;3(1):10. doi:10.3978/j.issn.2305-5839.2014.11.03
55. Lindsetmo RO, Johnsen R, Eide TJ, Gutteberg T, Husum HH, Revhaug A. Accuracy of *Helicobacter pylori* serology in two peptic ulcer populations and in healthy controls. *World J Gastroenterol WJG*. 2008;14(32):5039-5045. doi:10.3748/wjg.14.5039
56. Raj P, Thompson JF, Pan DH. *Helicobacter pylori* serology testing is a useful diagnostic screening tool for symptomatic inner city children. *Acta Paediatr Oslo Nor 1992*. 2017;106(3):470-477. doi:10.1111/apa.13724
57. Jara MG, Benso B, Lagos MJ, Tapia PC, Paulino MB, Silva CI. PCR-detection of *Helicobacter pylori* from oral mucosa: A feasible early diagnostic tool. *Ann Diagn Pathol*. 2022;61:152022. doi:10.1016/j.anndiagpath.2022.152022
58. Taylor NS, Fox JG. Animal Models of *Helicobacter*-Induced Disease: Methods to Successfully Infect the Mouse. *Methods Mol Biol Clifton NJ*. 2012;921:131-142. doi:10.1007/978-1-62703-005-2_18
59. Wang YK, Kuo FC, Liu CJ, et al. Diagnosis of *Helicobacter pylori* infection: Current options and developments. *World J Gastroenterol WJG*. 2015;21(40):11221. doi:10.3748/wjg.v21.i40.11221

60. Yokota S ichi, Ohnishi T, Muroi M, Tanamoto K ichi, Fujii N, Amano K ichi. Highly purified *Helicobacter pylori* LPS preparations induce weak inflammatory reactions and utilize Toll-like receptor 2 complex but not Toll-like receptor 4 complex. *FEMS Immunol Med Microbiol.* 2007;51(1):140-148. doi:10.1111/j.1574-695X.2007.00288.x
61. Muotiala A, Helander IM, Pyhälä L, Kosunen TU, Moran AP. Low biological activity of *Helicobacter pylori* lipopolysaccharide. *Infect Immun.* 1992;60(4):1714-1716.
62. Song Z, Li B, Zhang Y, et al. Outer Membrane Vesicles of *Helicobacter pylori* 7.13 as Adjuvants Promote Protective Efficacy Against *Helicobacter pylori* Infection. *Front Microbiol.* 2020;11. Accessed May 1, 2023. <https://www.frontiersin.org/articles/10.3389/fmicb.2020.01340>
63. Liu Q, Li X, Zhang Y, et al. Orally administered outer-membrane vesicles from *Helicobacter pylori* reduce *H. pylori* infection via Th2-biased immune responses in mice. *Pathog Dis.* 2019;77(5). doi:10.1093/femspd/ftz050
64. Halder P, Maiti S, Banerjee S, et al. Bacterial ghost cell based bivalent candidate vaccine against *Salmonella Typhi* and *Salmonella Paratyphi A*: A prophylactic study in BALB/c mice. *Vaccine.* 2023;41(41):5994-6007. doi:10.1016/j.vaccine.2023.08.049
65. Banerjee S, Halder P, Das S, et al. Pentavalent outer membrane vesicles immunized mice sera confers passive protection against five prevalent pathotypes of diarrheagenic *Escherichia coli* in neonatal mice [published online ahead of print, 2023 Sep 19]. *Immunol Lett.* 2023;263:33-45. doi:10.1016/j.imlet.2023.09.009
66. Lu H, Hsu PI, Graham DY, Yamaoka Y. Duodenal ulcer promoting gene of *Helicobacter pylori*. *Gastroenterology.* 2005 Apr;128(4):833-48. doi: 10.1053/j.gastro.2005.01.009. PMID: 15825067; PMCID: PMC3130061.
67. Margherita Coccia, Oliver J. Harrison, Chris Schiering, Mark J. Asquith, Burkhard Becher, Fiona Powrie, Kevin J. Maloy; IL-1 β mediates chronic intestinal inflammation by promoting the accumulation of IL-17A secreting innate lymphoid cells and CD4⁺ Th17 cells. *J Exp Med* 27 August 2012; 209 (9): 1595–1609. doi: <https://doi.org/10.1084/jem.20111453>

Figures

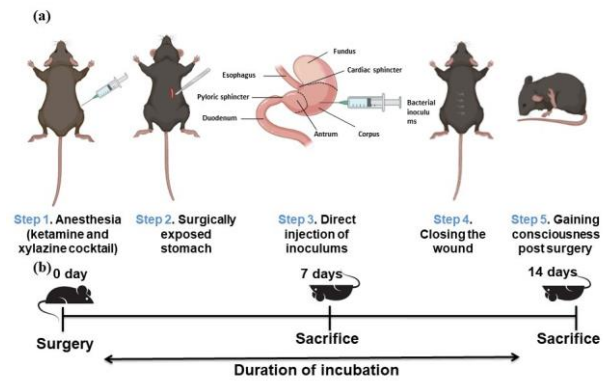


Fig. 1. Schematic diagram of the intragastrically infection model in C57BL/6 mice. (a) Graphical Representation of the “Surgical Model” using C57BL/6. Bacterial inoculation ($\sim 2 \times 10^8$ CFU/mL) is directly injected into the stomach, **(b)** Schematic schedule from infection to sacrifice.

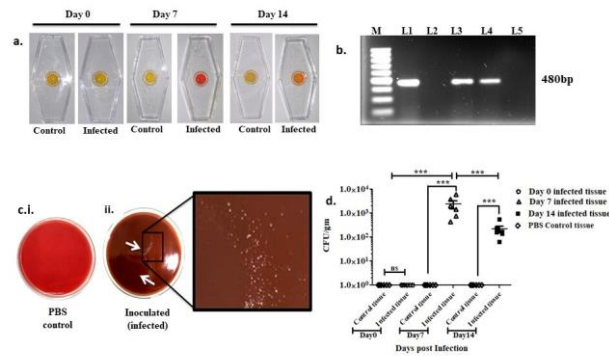


Fig. 2. Intra-gastric infection induced by wild type (WT) SS1 observed through urease test, *ureB* PCR, colonization in gastric tissue. (a) RUT of infected gastric tissue; Day 0, Day7 and Day 14 with respective PBS control, (b) Confirmatory *ureB* PCR for the presence of *H. pylori* recovered from the gastric tissue of infected mice. M-100bp marker, L1-positive control, L2-day 0 post infection, L3-day7 post infection, L4-14-day post infection, L5-PBS control. (c) Blood agar plates showing (c.i.) plate containing no *H. pylori* colonies recovered from gastric tissue of 7days post PBS inoculated mice (c.ii) plate containing *H. pylori* colonies recovered from gastric tissue of 7days post SS1 infected mice. (d) Colonies recovered from mice of 0, 7- and 14-days post infection. Data represented here are the mean values +/-Standard Deviation (SD) of three independent experiments. The differences in day wise response of each colonization assay were highly significant with respect to PBS control tissue. Statistical significance was found between 0day, 7day and 14day infected mice tissue (*p<0.001, ns-non-significant).**

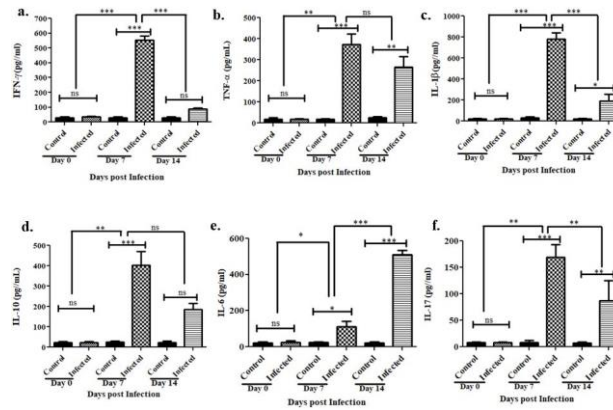


Fig. 3. *Helicobacter pylori*; wild type (WT) SS1 induces the production of cell mediated cytokines responses post-surgical intervention. (a) IFN- γ , (b) TNF- α , (c) IL-1 β , (d) IL-10, (e) IL-6, (f) IL-17 cytokines in serum isolated on Day 0, Day 7 and Day 14 post-surgical infection with respective PBS controls. All cytokines are measured by ELISA (n = 6). Statistical analyses were performed using the non-parametric Student's *t* test (Mann-Whitney tests) to evaluate data; (***)p value < 0.001, (**)p value < 0.01, (*)p value < 0.05, ns=Non-significant), Each bar represents median and error values of Six \pm SE of three independent experiments.

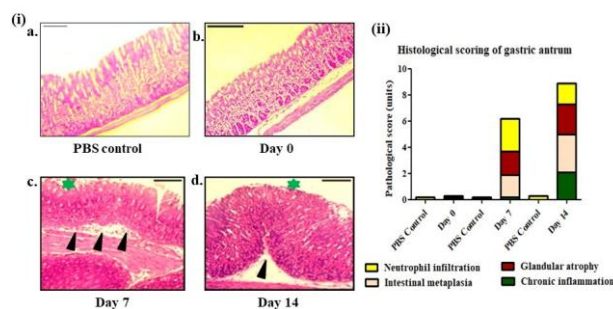


Fig. 4. Histological (H&E staining) observation and histological scoring of gastric epithelium after intragastric surgical infection with *Helicobacter pylori* (SS1). (i) a, b, c, d; all are the antrum part of the stomachs harvested from C57BL/6 mice. (i.a) no distinct changes observed in PBS control, mice receiving PBS only, (i.b) zero inflammation in Day 0 post-surgical infection of C57BL/6 mice, (i.c) severe inflammatory cell infiltration, glandular atrophy, intestinal metaplasia of 7 days post-surgical infection of C57BL/6 mice, (i.d) mild to moderate inflammatory cell infiltration, disruption in epithelial lining, glandular atrophy, chronic inflammation in 14 days post-surgical infection of C57BL/6 mice. Images were captured at 20 \times magnification. Scale bar represents 100 μ m. Inflammatory cell infiltration indicated by (black arrowhead), gastric epithelial damage (green star); (ii) Histopathological scoring is done according to Huston updated Sydney classification system. Colored histogram represents the mean scores of histological scoring of experimental animals (n=6) and PBS controls (n=6). All experiments were performed in triplicate.

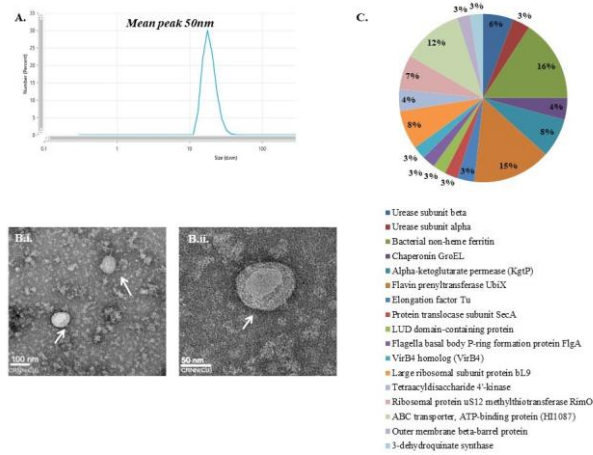


Fig. 5. Characterization of *Helicobacter pylori* OMVs isolated from strain A61C (1); (A) Dynamic Light Scattering showing a uniformity in OMVs population with mean peak at 50nm, (B) Transmission Electron microscopy images revealing the circular morphology of *Helicobacter pylori* OMVs of A61C (1) strain; (B.i) Image taken at 100nm scale, (B.ii) Image taken at 50nm scale. Both TEM images revealed the thick bilayer structure with hollow center of the OMVs. (C) Percentage of major proteins present on OMVs.

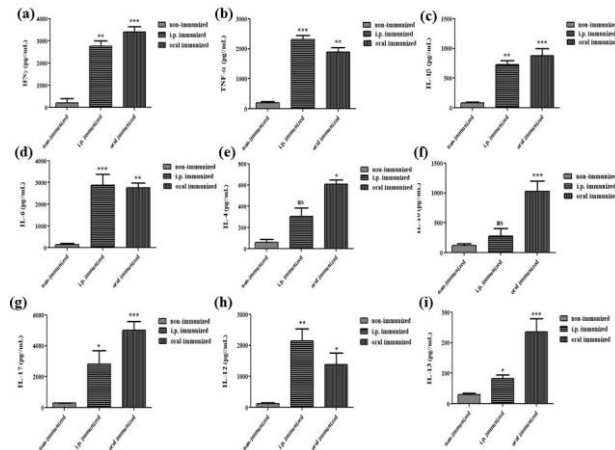


Fig. 6. *Helicobacter pylori* OMVs induces the production of cell mediated cytokines responses. (a) IFN- γ , (b) TNF- α , (c) IL-1 β , (d) IL-6, (e) IL-4, (f) IL-10, (g) IL-17, (h) IL-12, (i) IL-13, cytokines in culture supernatant of ex-vivo cultured splenic cells of immunized and non-immunized (PBS immunized) mice after 24 h of re-stimulation with OMVs. The differences in immunized (i.p. and oral immunization) mice serum response of each of the studied cytokines were highly significant than nonimmunized. All cytokines are measured by ELISA (n = 6). Statistical analyses were performed using the non-parametric Student's *t* test (Mann-Whitney tests) to evaluate data; (***)p value <0.001, (**)p value <0.01, (*)p value <0.05, ns=Non-significant). Each bar represents median and error values of six \pm SE of three independent experiments.

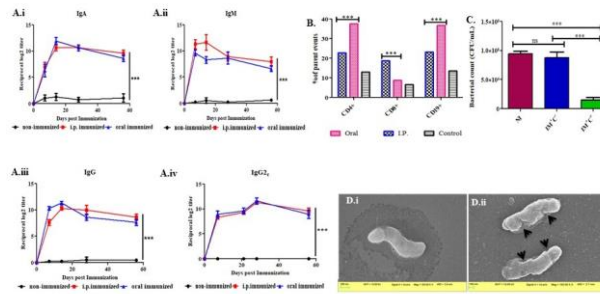


Fig. 7. Reciprocal log₂ titer of serum IgA, serum IgM, serum IgG, and serum IgG2c immunoglobulins from *Helicobacter pylori* OMVs immunized and non-immunized (PBS immunized) group against OMPs. Immunization induces the population of CD4+, CD8+, and CD19+ splenic cells of immunized over non-immunized (PBS immunized) mice and the microscopic image of serum bactericidal activity of immunized and non-immunized. Mouse serum IgA (A.i), serum IgM (A.ii), serum IgG (A.iii), serum IgG2c (A.iv) was measured separately after three doses of intraperitoneal or oral immunization against Outer membrane protein (OMP) of *Helicobacter pylori*. (B) Bar diagram represents the percentage of CD 19+, CD 4+, and CD 8+ splenic cells from immunized and non-immunized mice using FACS analyses. Significant statistical difference was found between OMVs immunized and non-immunized spleen cell population (***) p value < 0.001). (C) OMVs immunized mouse serum is effective in complement mediated lysis of *H. pylori* (SS1). *H. pylori* (SS1) was separately incubated with OMVs immunized serum or non-immunized serum with or without guinea pig complement for 1 h at 37 °C. Viable bacterial count was determined by spread-plate method. Two-way analysis of variance (ANOVA) test was used for statistical analysis. Bars represent mean ± S.E. of three individual experiments. (***) p value < 0.001, ns-Non-significant). NI, non-immunized serum; IM+C-, OMVs immunized serum without complement; IM+C+, OMVs immunized serum with complement. (D) Scanning electron microscopic images after Serum Bactericidal Assay using non-immunized serum with complement (i) and immunized serum with complement (ii) (black arrowheads indicate immunized antibody-mediated lysis in presence of complement).

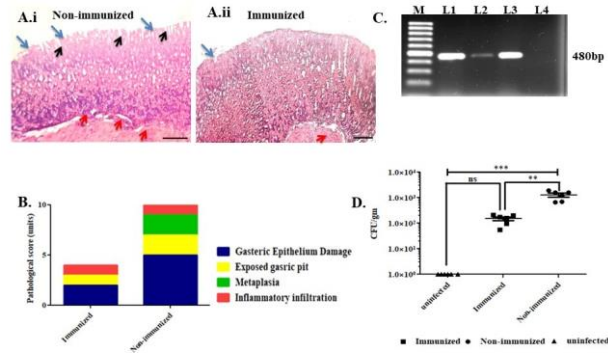


Fig. 8. OMVs immunized mice shows reduced gastric tissue damage, inflammation after infection with SS1 (2×10^8 CFU) and reduce bacterial colonization in gastric tissue. Histological images represent both (A.i) non-immunized (PBS immunized) antrum of stomach and (A.ii) immunized antrum of stomachs. OMVs immunized mice showed mild epithelial layer damage, less altered gastric mucosa and inflammatory infiltration, whereas non-immunized mice displayed marked epithelial damage, inflammatory infiltration, exposed gastric pit and early signs of gastric metaplasia. (Blue arrow: gastric epithelium; Black arrow: exposed gastric pit; Red arrow: Inflammatory infiltration) (B) Pathological scores of immunized or non-immunized mice post *Helicobacter pylori* SS1 challenge. (C) *ureB* PCR shows significant changes in bacterial DNA yield harvested from gastric tissues of both non-immunized and immunized mice post intragastric surgical challenge; M: 100bp ladder, L1: Positive control, L2: Immunized mice gastric tissue, L3: Non-immunized mice gastric tissue, L4: Negative control (D) *Helicobacter pylori* colonization in gastric tissue of immunized and non-immunized mice 7 days post challenge.

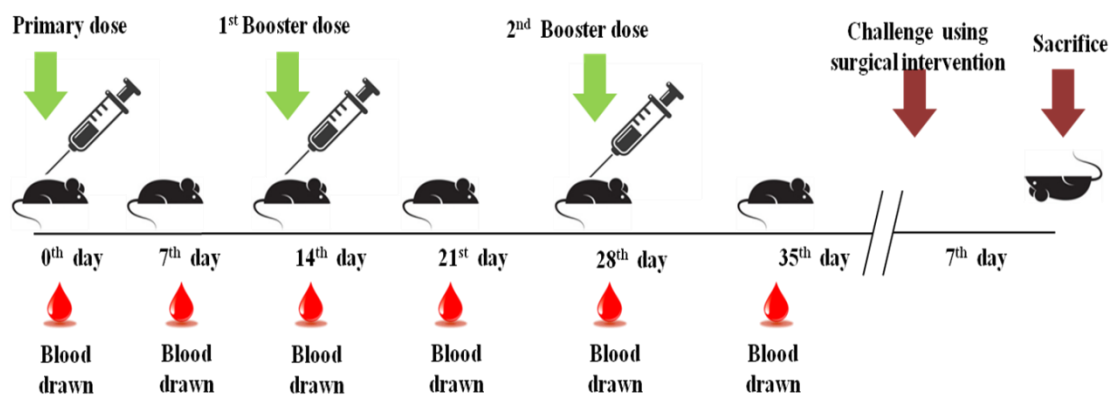


Fig. S1. Immunization and blood collection schedule Oral or Intraperitoneal (i.p.) route of immunization

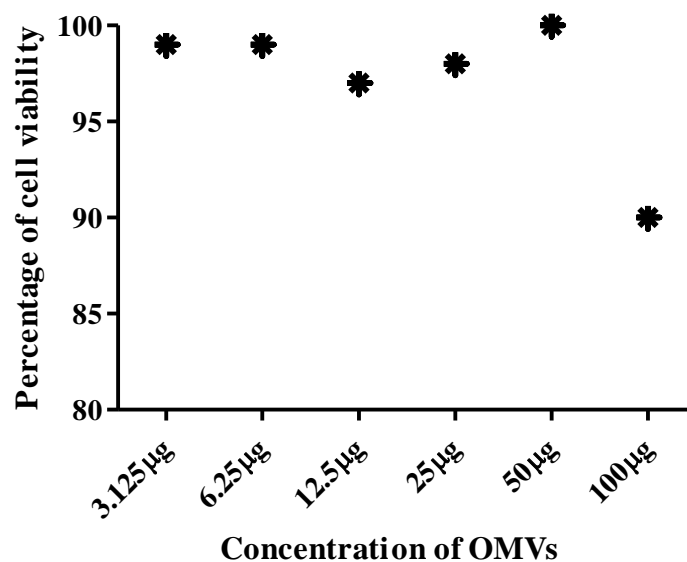


Fig. S2. *in-vitro* cytotoxicity test with different concentrations of OMVs

Table S1. The Antibiotic profile of *Helicobacter pylori* used for immunogen strain selection.

Strains			Antibiotics					
			Clarithromycin		Amoxicillin		Metronidazole	
			S	R	S	R	S	R
1	Ref. strains	26695	+	-	+	-	-	+
		J99	+	-	+	-	-	+
		SS1	+	-	+	-	-	+
2	BHU 8A		-	+	+	-	-	+
3	KO 8A		+	-	+	-	-	+
4	AS 2		+	-	+	-	-	+
5	OT-10 (A)		+	-	+	-	-	+
6	B34		+	-	+	-	-	+
7	D383		+	-	+	-	-	+
8	B6		+	-	+	-	-	+
9	M28		+	-	+	-	-	+
10	L7		+	-	+	-	-	+
11	A61C(1)		+	-	+	-	-	+
12	AM1		+	-	+	-	-	+
S - sensitive					R - resistant			

Table S2. Primers of specific genes of *Helicobacter pylori* used in this study.

Gene Assigned	Primer	Sequence	Amplicon (bp)	Reference
<i>cagA</i>	cag5c-F cag3c-R	5'-GTTGATAACGCTGTCGCTTCA-3' 5'-GGGTTGTATGATATTTTCCATAA-3'	350	Chattopadhyay et al, 2004 [20]
<i>vacA s1/s2</i>	VA1-F VA1-R	5'-ATGGAAATACAACAAACACAC-3' 5'-CTGCTTGAATGCGCCAAAC-3'	259/286	
<i>vacA m1/m2</i>	VAG-F VAG-R	5'-CAATCTGTCCAATCAAGCGAG-3' 5'-GCGTCAAATAATTCCAAGG-3'	567/642	
<i>babA2</i>	babA2R babA2F	5'-AATCCAAAAAGGAGAAAAAGTATGAAA-3' 5'-GTTTTCTTTGAGCGCGGGTAAGC-3'	607	Ghosh et al, 2016 [21]
<i>ureB</i>	ureBF ureBR	5'-CGTCCGGCAATAGCTGCCATAGT-3' 5'-GTAGGTCCTGCTACTGAAGCCTTA-3'	480	Ghosh et al, 2016 [21]
<i>dupA</i>	jhp0917F jhp0917R	5'-TGGTTTCTACTGACAGAGCGC-3' 5'-AACACGCTGACAGGACAATCTCCC-3'	307	Lu et al, 2005 [66]
	jhp0918F jhp0918R	5'-CCTATATCGCTAACGCGCGCTC-3' 5'-AAGCTGAAGCGTTTGTAACG-3'	276	
<i>16SrRNA</i>	16SF 16SR	5'-CTGGAGAGACTAAGCCCTCC-3' 5'-ATTACTGACGCTGATTGCGC-3'	110	Kashyap et al., 2020 [67]

Table S3. Result of major virulence genes of *Helicobacter pylori* screened for immunogen strain selection

Genetic Features			Virulence Marker					Adhesion	Duodenal Ulcer Promoting Gene	
Strains			<i>cagA</i>	<i>vacA</i>				<i>babA2</i>	<i>dupA</i>	
				<i>s1</i>	<i>s2</i>	<i>m1</i>	<i>m2</i>		<i>jhp0917</i>	<i>jhp0918</i>
1	Ref. strains	26695	+	+	-	+	-	-	-	-
		J99	+	+	-	+	-	+	+	+
		SS1	+	-	+	-	+	-	-	-
2	BHU 8A		+	+	-	-	+	+	-	-
3	KO 8A		+	+	-	+	-	+	-	-
4	AS 2		+	+	-	+	-	-	-	-
5	OT-10 (A)		+	+	-	+	-	-	-	-
6	B34		+	+	-	+	-	+	-	-
7	D383		-	-	+	-	+	-	-	-
8	B6		+	+	-	-	+	+	-	-
9	M28		+	+	-	-	+	-	-	-
10	L7		+	+	-	+	-	+	-	-
11	A61C(1)		+	+	-	+	-	+	+	+
12	AM1		-	-	+	-	+	-	-	-

Table S4. Proteomic analyses of OMVs isolated from *Helicobacter pylori* strain A61C(1).

Accession	Protein assigned	Molecular mass (kDa)	No. of peptides	Sequence coverage (%)
P69996	nickel cation binding, urease activity	61.6	3	7
P14916	nickel cation binding, urease activity	26.5	1	4
P52093	ferric iron binding, ferrous iron binding, ferroxidase activity	19.3	2	19
P42383	ATP binding, ATP-dependent protein folding chaperone, isomerase activity, unfolded protein binding	58.2	3	5
O25723	transmembrane transporter activity	47.5	1	9
O26011	carboxy-lyase activity, flavin prenyltransferase activity	20.6	1	18
P56003	GTP binding, GTPase activity, guanosine tetraphosphate binding, translation elongation factor activity	43.6	2	4
O25475	ABC-type protein transporter activity, ATP binding, metal ion binding, protein-exporting ATPase	99	1	3

	activity			
O24949	Hypothetical protein	23.6	1	3
O26012	Hypothetical protein	24.3	1	3
O25206	ATP binding, DNA binding	98.4	1	3
P56035	rRNA binding, structural constituent of ribosome	16.5	1	9
O25095	ATP binding, tetraacyldisaccharide 4'-kinase activity	35.5	1	5
O25434	4 iron, 4 sulfur cluster binding, aspartic acid methylthiotransferase activity, metal ion binding, protein methylthiotransferase activity	49.6	1	8
O26001	ATP binding, ATP hydrolysis activity	29.2	1	14
O25992	Hypothetical protein	82.3	1	3
P56081	3-dehydroquinate synthase activity, metal ion binding, nucleotide binding	39.1	1	3

Table S5. Sydney classification of histopathological scoring used in the study

	Neutrophil infiltration	Glandular atrophy	Intestinal metaplasia	Chronic inflammation
Grade I	<1/3 of surface infiltrated	Mild	<1/3 of surface infiltrated	5-10 cells x 40
Grade II	1/3- 2/3 of surface infiltrated	Moderate	1/3- 2/3 of surface infiltrated	11-20 cells x 40
Grade III	>2/3 of surface infiltrated	Severe	>2/3 of surface involved	>21cells x 40

Scores assigned: mild=1, moderate=2, severe=3

Table S6. List of Antibodies used in the study

Sl no.	Antibody	Catalog no	Company
1.	Anti mouse-IgA	AB97235	Abcam
2.	Anti mouse-IgG2c	AB97255	Abcam
3.	Anti mouse-IgG	AB97023	Abcam
4.	Anti mouse-IgM	A8786	Sigma aldrich

Table S7.

Available for download at

<https://journals.biologists.com/bio/article-lookup/doi/10.1242/bio.060282#supplementary-data>